CHAPER 3

NOISE SUPPRESSION IN REAL DATA APPLICATION

This chapter was shown and analyzed results of SVD, f-x prediction and 2-D median filters on seismic and GPR data. For seismic data, the filters were inserted into processing steps at 4 positions for efficiency test of filter in each step of processing. For GPR data, the filters were applied at the final step of processing.

3.1 Seismic data sets

The experiments were adapted on a seismic shot record (#533), a CDP gather (#1072), a NMO corrected CDP supergather (#1072) and final stack section with residual static correction. Each experiment, singular value spectrum was plotted and SVD filter was applied. The f-x predictive and 2-D median filters also were applied on the same data set. The ground roll, air waves, random noise and reflectors were used to indicate noise suppression efficiency of each images. The images quality depends on ground roll, air waves and random noise attenuations which reflectors were appeared.

The processing steps in Figure 3-1 was stages of basic processing which comprised of f-k filter, band pass filter, predictive decovolution, NMO correction and stack. The f-k filter of 0-500 m/s fan shape was applied to eliminate the ground roll (Figure 3-2). The f-k filter was processed again after NMO correction which 0-2500 m/s fan shape was applied to eliminate the random noise (Figure 3-3).

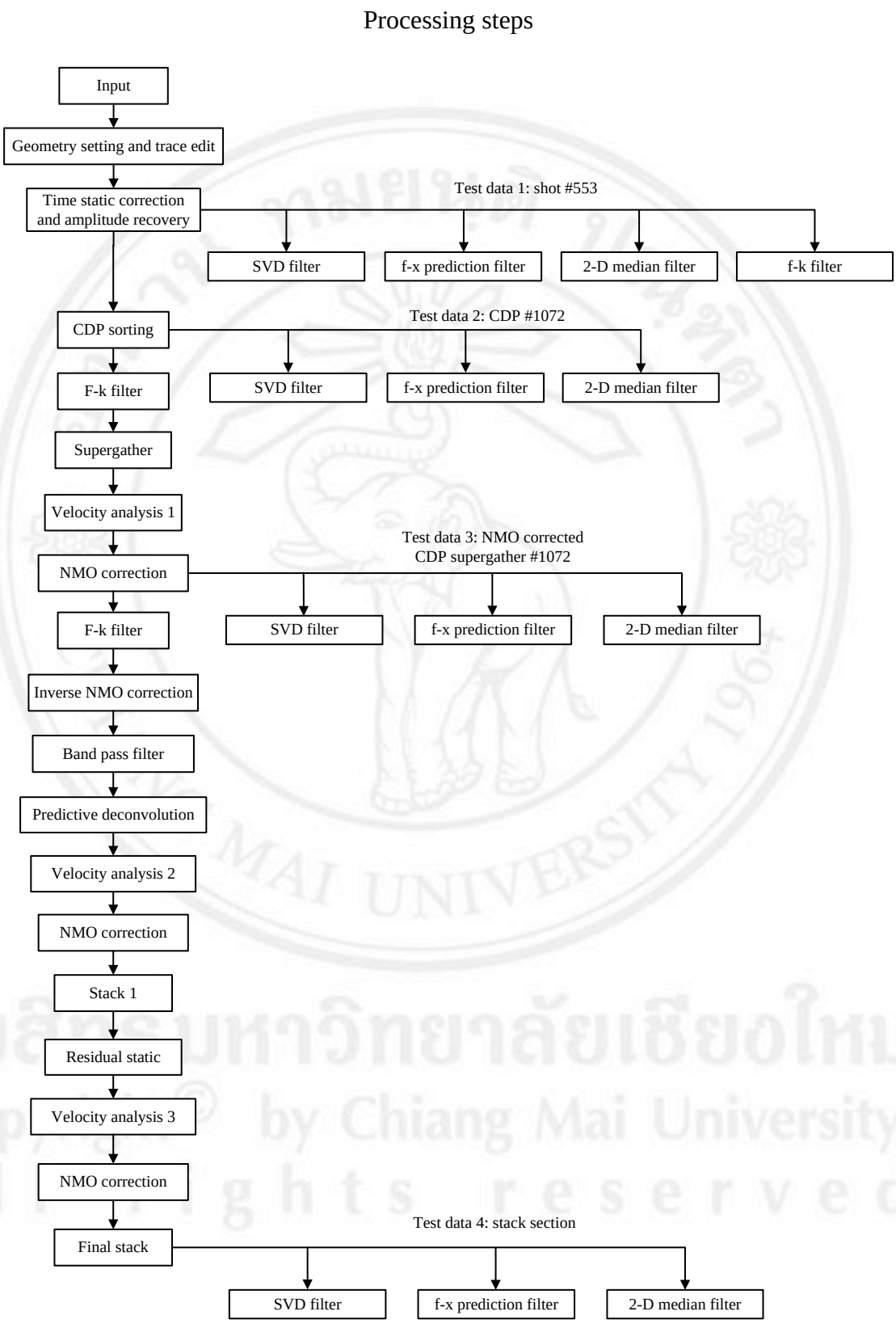

Figure 3-1. Flowchart of seismic processing.

Table 3-1 Processing steps (A) and parameters of seismic data.

Processing	Parameters/remark
1. Geometry setting and trace edit	
2. Time static and amplitude correction	mean scale; (test in data set 1: shot gather)
3. F-k filter	0-500 m/s fan shape
4. CDP sorting	(test in data set 2: CDP gather)
5. Supergather	3 CDP to 1 supergather
6. Velocity analysis 1	
7. NMO correction	(test in data 3: NMO correction CDP gather)
8. F-k filter	0-2500 m/s fan shape
9. Inverse NMO correction	
10. Band pass filter	15-25-80-90 Hz
11. Predictive deconvolution	2^{nd} crossing, n = 30 ms, ε = 0.1%
12. Velocity analysis 2	
13. Stack 1	brute stack section
14. Residual static correction	
15. Velocity analysis 3	
16. Final stack	final stack section of basic processing; (test in data 4: stack section)

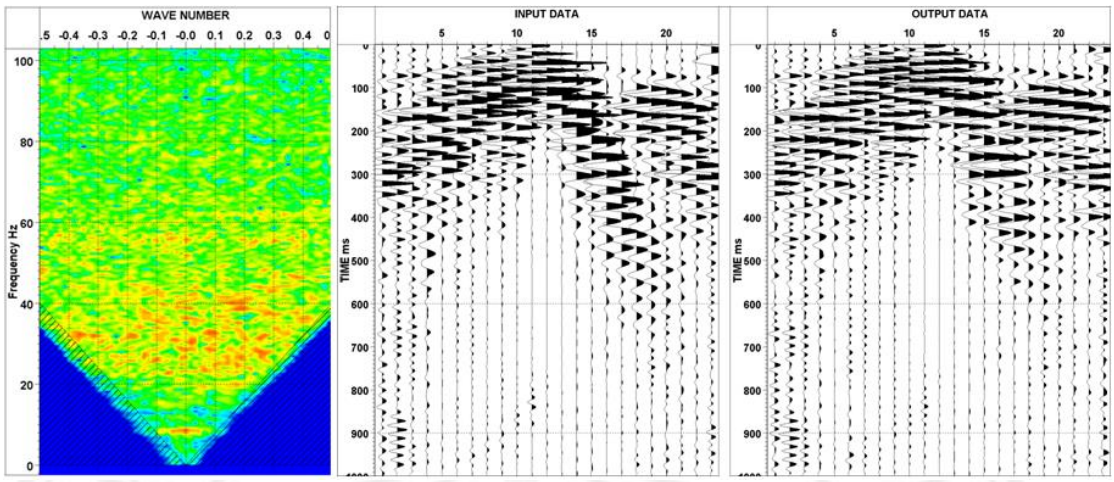

Figure 3-2. (left) The f-k filter of 0-500 m/s fan shape, (middle) before f-k filter and (right) after f-k filter.

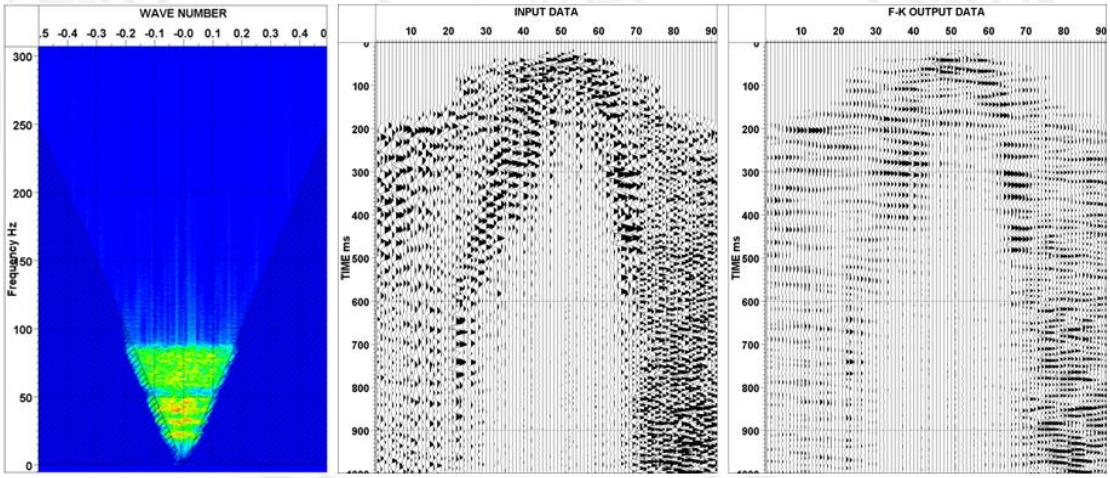

Figure 3-3. (left) The f-k filter of 0-2500 m/s fan shape, (middle) before f-k filter and (right) after f-k filter.

3.1.1 Tested data 1: Shot gather (#533)

The singular value spectrum of a shot gather in Figure 3-4 was illustrated the slope characteristic. Based on the slope, the singular value spectrum can be divided into 3 parts as follows by p=1 to q=4, p=4 to q=11 and p=11 to q=31. A shot gather was displayed in Figure 3-5a. It contains coherent noises such as ground roll and airwaves. Figure 3-5b presented some flat event. Figure 3-5c presented ground roll without airwaves and reflectors. Figure 3-5d illustrated partially ground roll and airwaves elimination.

The comparison of the images quality was described as follows; the ground roll, air waves, random noise and reflectors was removed in Figure 3-5b. The air waves were removed, the some part of ground roll was remained and reflectors were not appeared in Figure 3-5c. The some part of ground roll, air waves and random noise was remained which reflectors were preserved in Figure 3-5d. The Figure 3-5d was the best image quality.

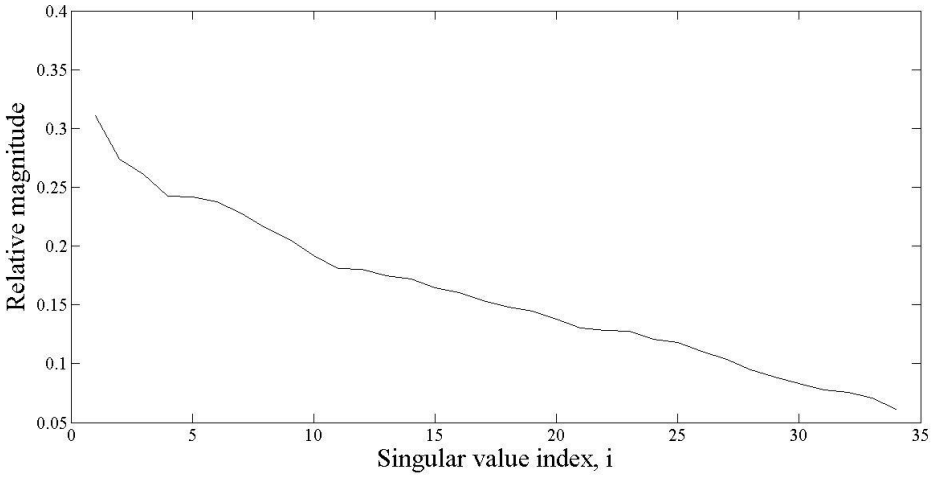

Figure 3-4. Singular value spectrum of a shot gather record number 533.

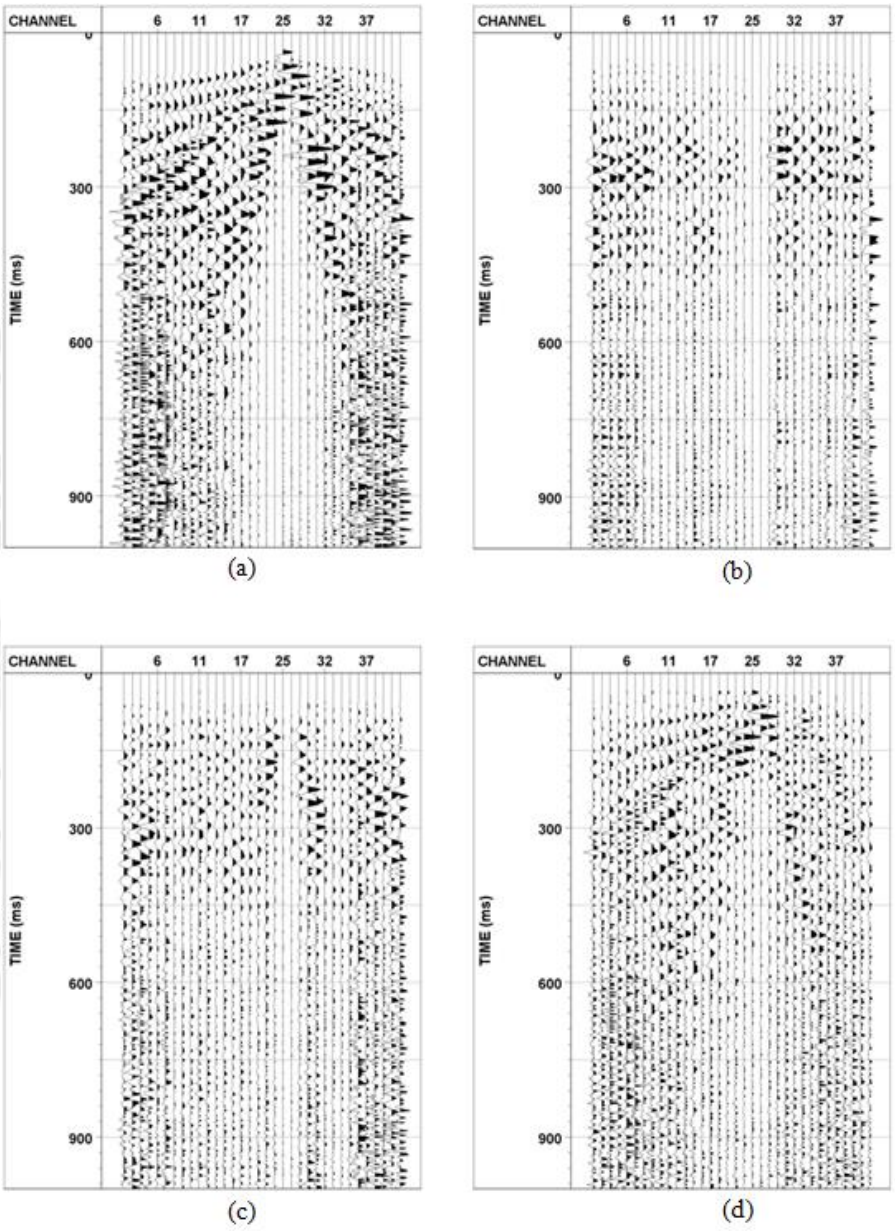

Figure 3-5. (a) A raw shot gather (b) A shot gather with SVD filter using p=1 to q=4. (c) A shot gather with SVD filter using p=4 to q=11. (d) A shot gather with SVD filter using p=10 to q=31.

The comparison results of SVD, f-x prediction, 2-D median and f-k filters can be seen in Figures 3-6a to 3-6d. Figure 3-6a shown that the ground roll and airwaves were nearly suppressed but random noises still remained. Figure 3-6b illustrated the partial airwave removal while ground roll still appeared. Figure 3-6c showed random

noises attenuation and most of the signal was distorted. Figure 3-6d indicated some high amplitudes noise removal.

From the comparison, the SVD filter is suitable to apply on raw shot gather. This filter can be removed some part of ground roll and air waves which reflectors were not attenuated.

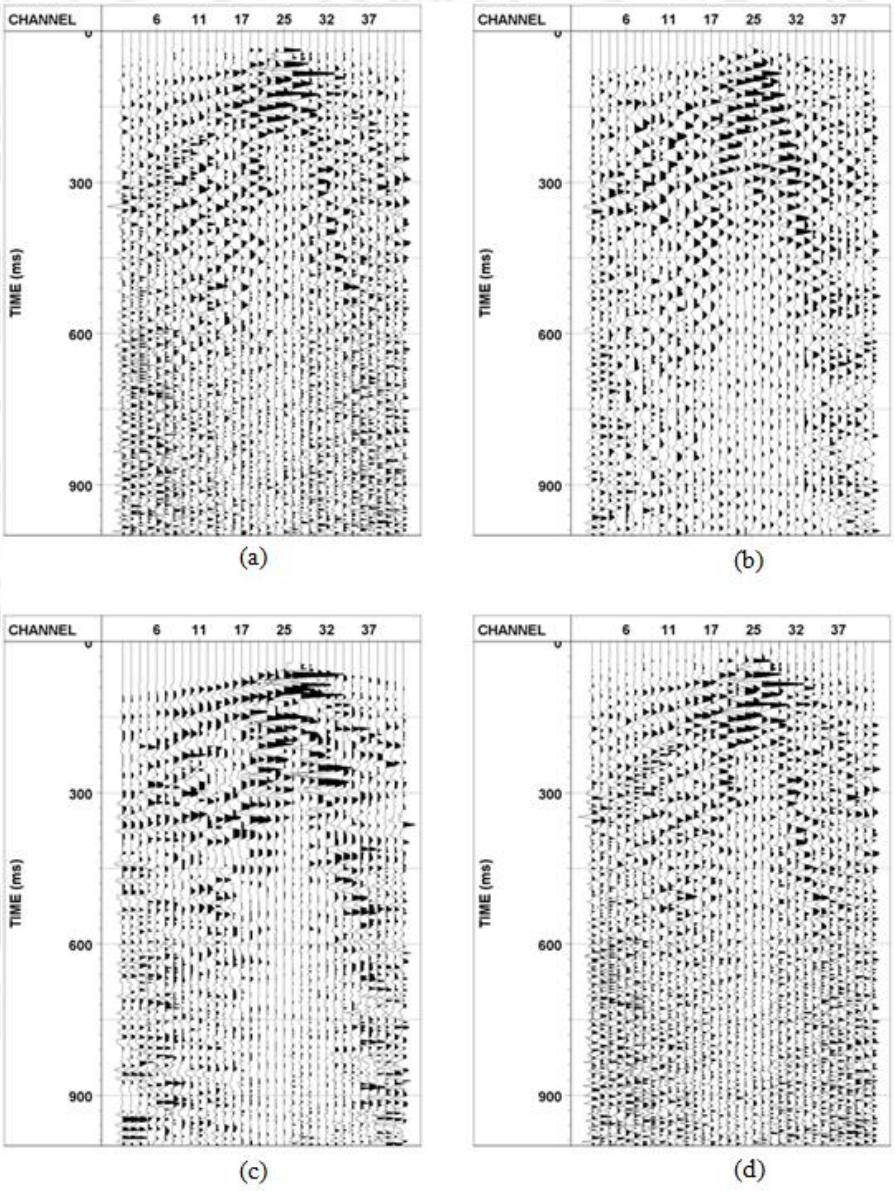

Figure 3-6. The comparison result of (a) SVD filter with p=10 to q=31, (b) f-x prediction filter with filter length of 4 traces and design windows of 15 traces, (c) 2-D median filter with window length of 2 traces and 3 samples and (d) f-k filter of 0-500 m/s fan shape.

3.1.2 Tested data set 2: CDP gather (#1072)

The singular value spectrum of CDP gather was shown in Figure 3-7. The spectrum can be divided into 3 parts; p=1 to q=3, p=3 to q=20 and p=10 to q=20. A CDP gather was displayed in Figure 3-8a. Figure 3-8b contaminated high and low amplitudes of flat events. Figure 3-8c shown some reflector but high amplitudes noise still remained. Figure 3-8d presented the reflectors distortion.

The each images of SVD filter found that the Figure 3-8c is the best images. The reflectors in Figures 3-8b and 3-8d were removed which the Figures 3-8c can be seen reflector at 280 ms and multiples can be seen at 340 ms and 450 ms.

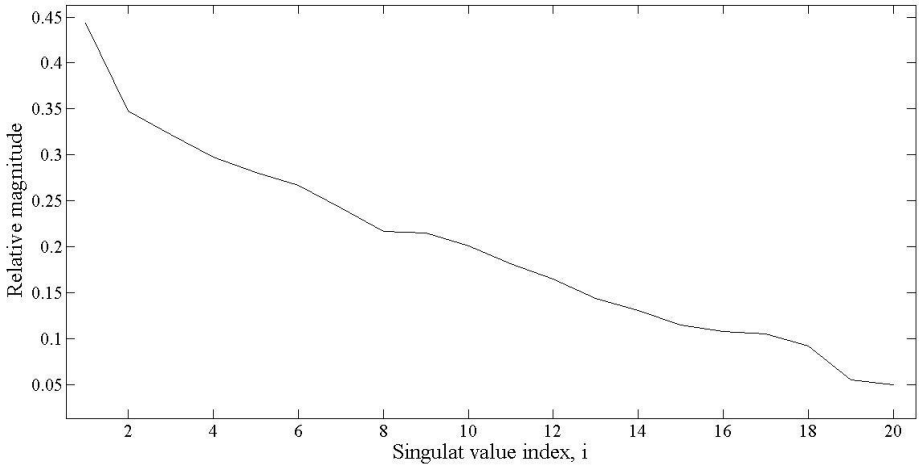

Figure 3-7. Singular value spectrum of a CDP gather number 1072.

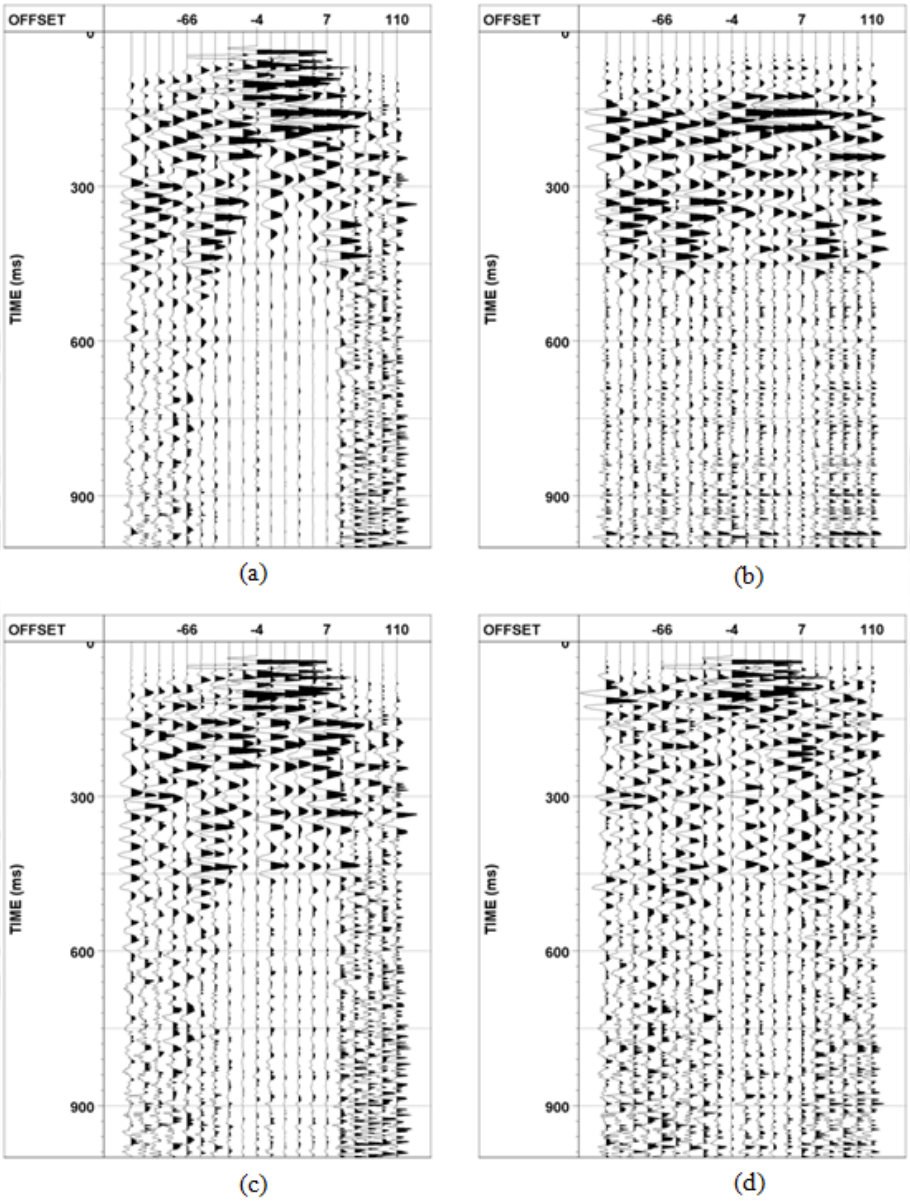

Figure 3-8. (a) A raw CDP gather (b) A CDP gather with SVD filter using p=1 to q=3. (c) A CDP gather with SVD filter using p=3 to q=20. (d) A CDP gather with SVD filter using p=10 to q=20.

The comparison results of SVD, f-x prediction, 2-D median filters and f-k filters can be seen in Figures 3-9a to 3-9d. Figure 3-9a and Figure 3-9d showed the most high amplitude noise reduction, hyperbolic events (red arrow) and multiples (blue arrows). Figure 3-9b and Figure 3-9c showed random noise suppression.

From the comparison, the SVD and f-k filters are suitable to apply on raw CDP gather, because the reflectors and multiples presented in both of profiles.

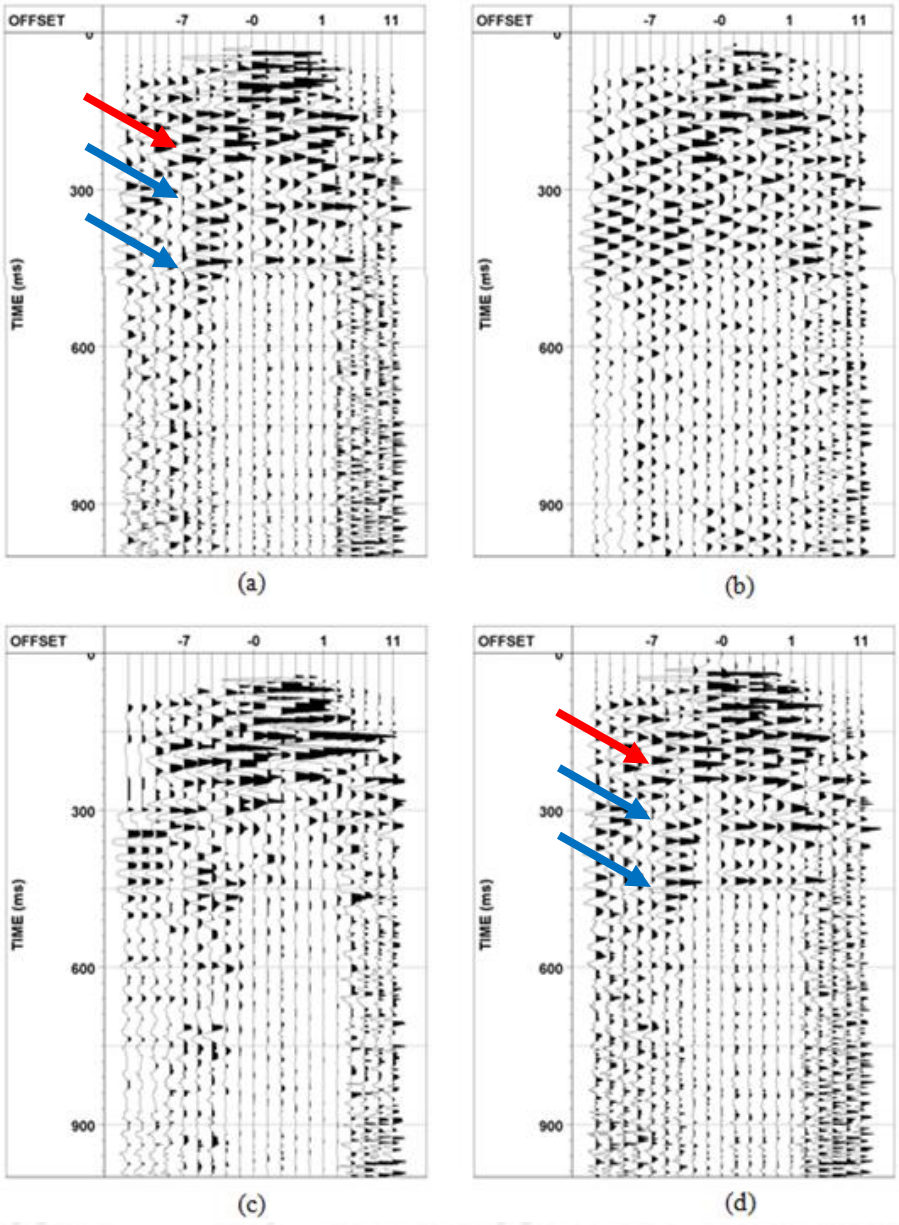

Figure 3-9. The comparison result of (a) SVD filter with p=3 to q=20, (b) f-x prediction filter with filter length of 4 traces and design windows of 9 traces, (c) 2-D median filter with window length of 2 traces and 3 samples and (d) f-k filter of 0-500 m/s fan shape.

3.1.3 Tested data set 3: NMO corrected CDP supergather (#1072)

The singular value spectrum of NMO corrected CDP supergather was displayed in Figure 3-10. The spectrum was divided into 3 parts; p=1 to q=7, p=7 to q=30 and p=30 to q=91. A NMO corrected CDP supergather consisting of 91 traces was presented in Figure 3-11a. Figure 3-11b contained high and low amplitudes of flat events. Figure 3-11c showed coherent noise attenuation and random noise. Figure 3-11d displayed only random noise.

The each images of SVD filter shown that the Figure 3-11c is a best the images quality. The images of Figure 3-11b and Figure 3-11d cannot be identified the reflectors.

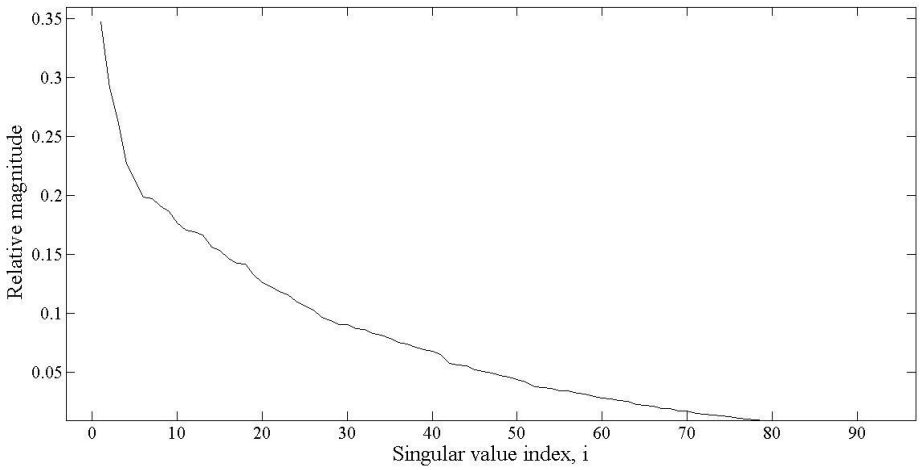

Figure 3-10. Singular value spectrum of a NMO corrected CDP supergather number 1072.

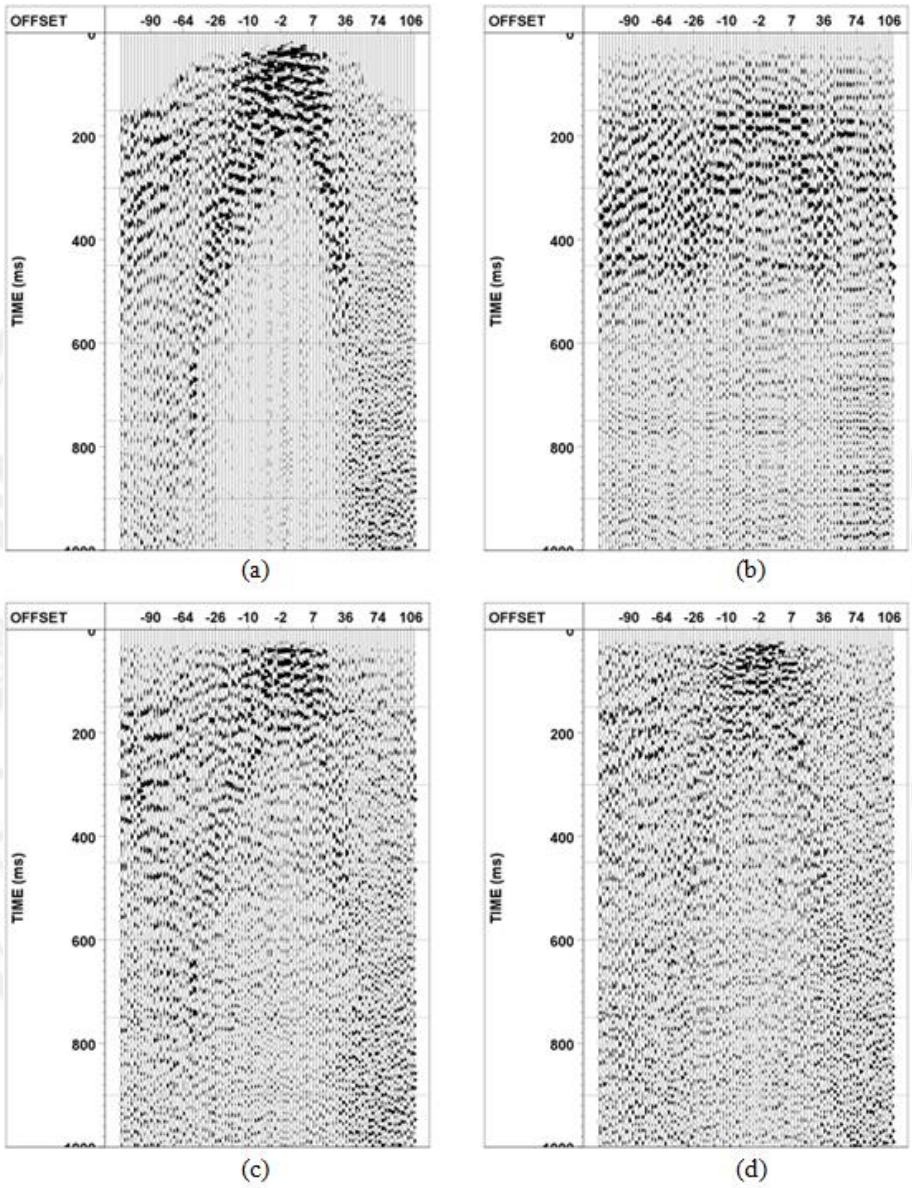

Figure 3-11. (a) A raw NMO corrected CDP supergather. (b) A NMO corrected CDP supergather with SVD filter using p=1 to q=7. (c) A NMO corrected CDP supergather with SVD filter using p=7 to q=30. (d) A NMO corrected CDP supergather with SVD filter using p=30 to q=91.

Figures 3-12a to 3-12d had shown the results of SVD, f-x prediction, 2-D median and f-k filters, respectively. Figure 3-12a and Figure 3-12b shown the same results and random noise still remained. Figure 3-12c and Figure 3-12d presented the linear events and random noise suppression.

For reason, the SVD are suitable to apply on NMO corrected CDP gather, because the signal in Figure 3-12c and Figure 3-12d was distorted. Figure 3-12b was not presented the reflectors.

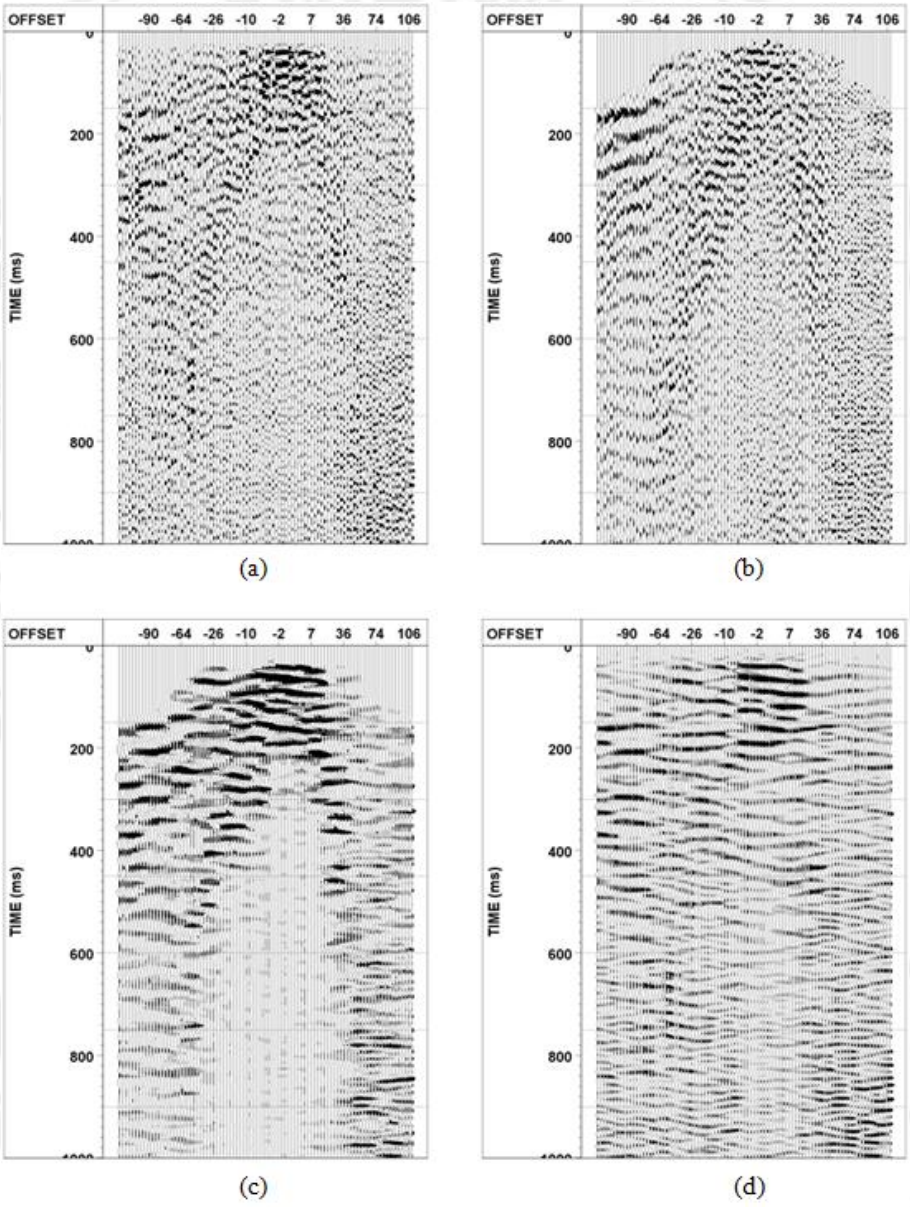

Figure 3-12. The comparison result of (a) SVD filter with p=7 to q=30, (b) f-x prediction filter with filter length of 4 traces and design windows of 48 traces, (c) 2-D median filter with window length of 5 traces and 3 samples and (d) f-k filter of 0-2500 m/s fan shape.

3.1.4 Tested data set 4: Stacked section

The singular value spectrum of the final stack section processed by processing flowchart in Figure 3-1 with residual static correction illustrated in Figure 3-13. The singular value spectrum can be divided into the 2 part; p=1 to q=15 and p=15 to q=140. The test used the parameters at the range of p=1 to q=15, p=1 to q=25 and p=1 to q=40. This test approximated relative magnitude 0.75 at q=40. The q value is not require to use q=140, because the relative magnitude value ~~at~~ last than 0.1±0.25 is not effect with filtering.

The final stack section with residual static correction was presented in Figure 3-14a. The section displayed the reflectors at 47 ms, 75 ms, 130 ms and 170 ms. Each result of SVD filter with random noise suppression. However~~,~~ reflectors at 120 ms to 200 ms of Figure 3-14c and Figure 3-14d were distorted. The Figure 3-14c is the best image quality.

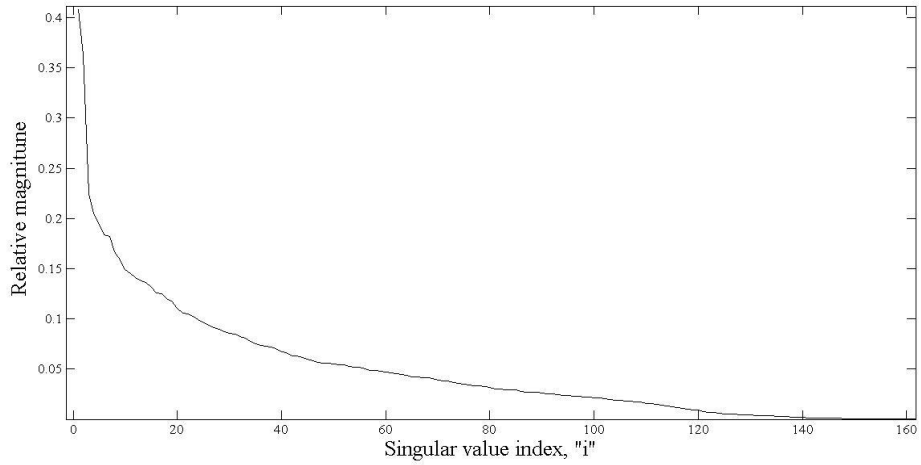

Figure 3-13. Singular value spectrum of the final stack section with residual static correction.

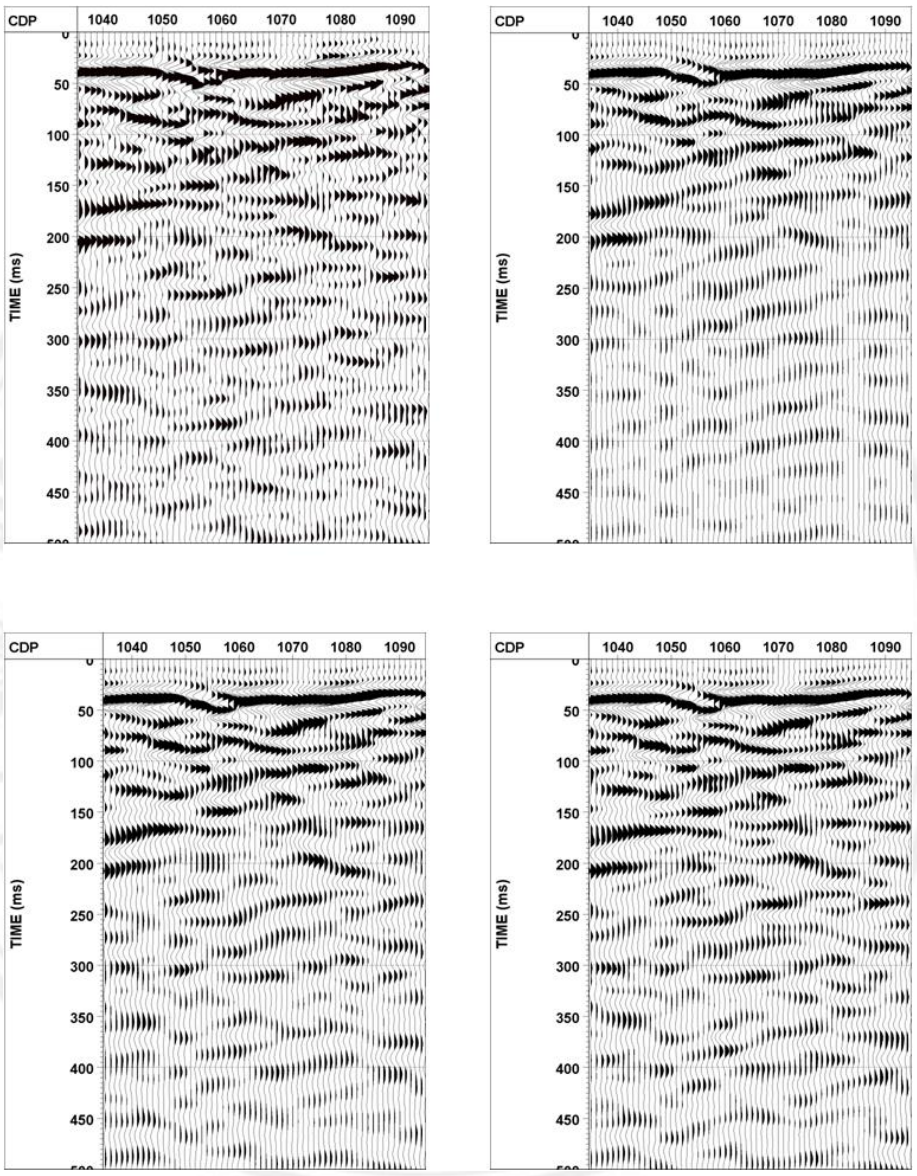

Figure 3-14. (a) The final stack section with residual static correction. (b) The final stack section with residual static correction with SVD filter using p=1 to q=15. (c) The final stack section with residual static correction with SVD filter using p=1 to q=25. (d) The final stack section with residual static correction with SVD filter using p=1 to q=40.

Figures 3-15a to 3-15c showed the results of SVD, f-x prediction and 2-D median filters applied on final stack section with residual static correction, respectively. Figures 3-15a and 3-15c were similar results and showed random noise elimination and reflector preservation. Figure 3-15b displayed the distortion of stack

section but the reflectors of f-x prediction filter were smooth more than the final stack section with residual static correction.

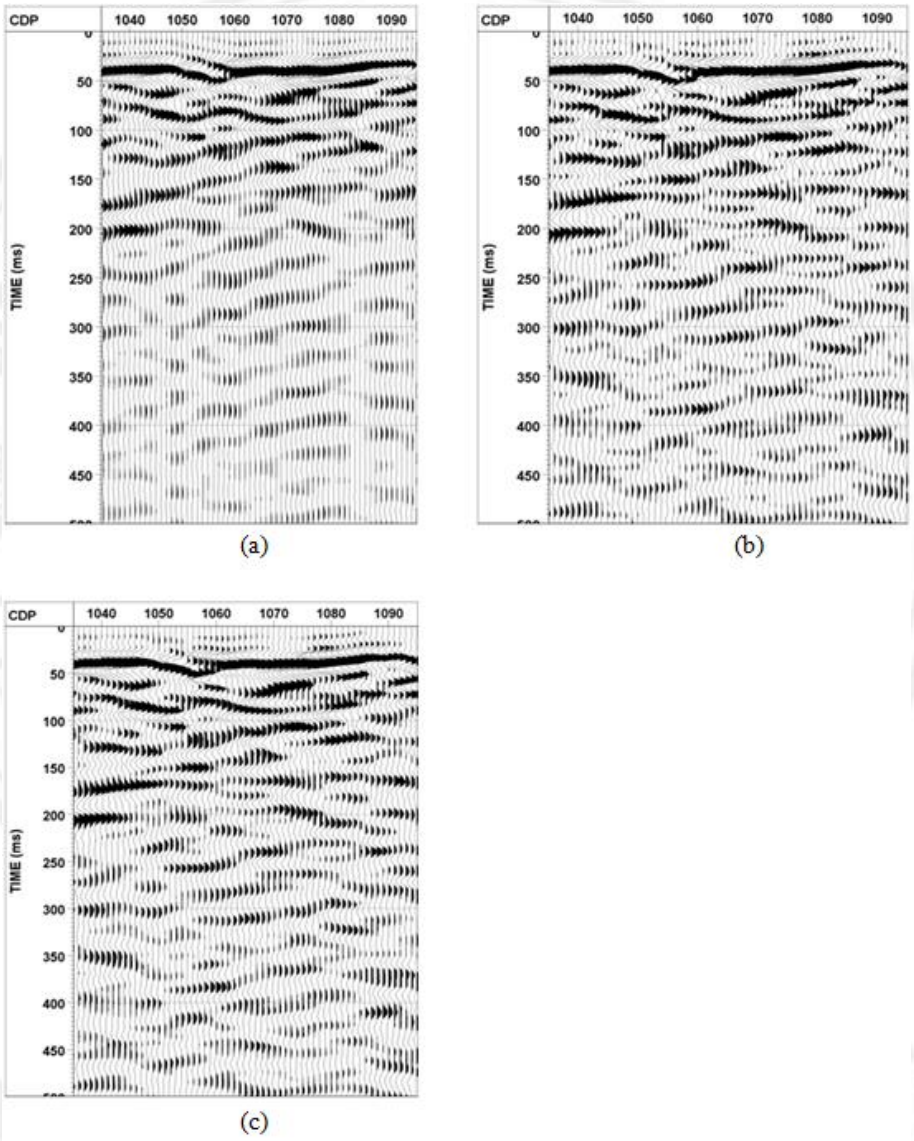

Figure 3-15. The comparison result of (a) SVD filter with p=1 to q=15, (b) f-x prediction filter with filter length of 4 traces and design windows of 48 traces, (c) 2-D median filter with window length of 5 traces and 3 samples.

3.2 GPR data set

The GPR data were selected into this investigation because anomaly is clearly seen and efficiency of filter is easily to observe. This can be observed from the present of hyperbolic events in the profile as an indicator of effectiveness of each filter.

The experiments were applied on GPR common offset gather. The GPR processing steps were displayed in Figure 3-16 and descriptions in Table 3-2. The filters were applied at the last processing step and compared the results of SVD filter with result of f-x predictive, 2-D median and f-k filters.

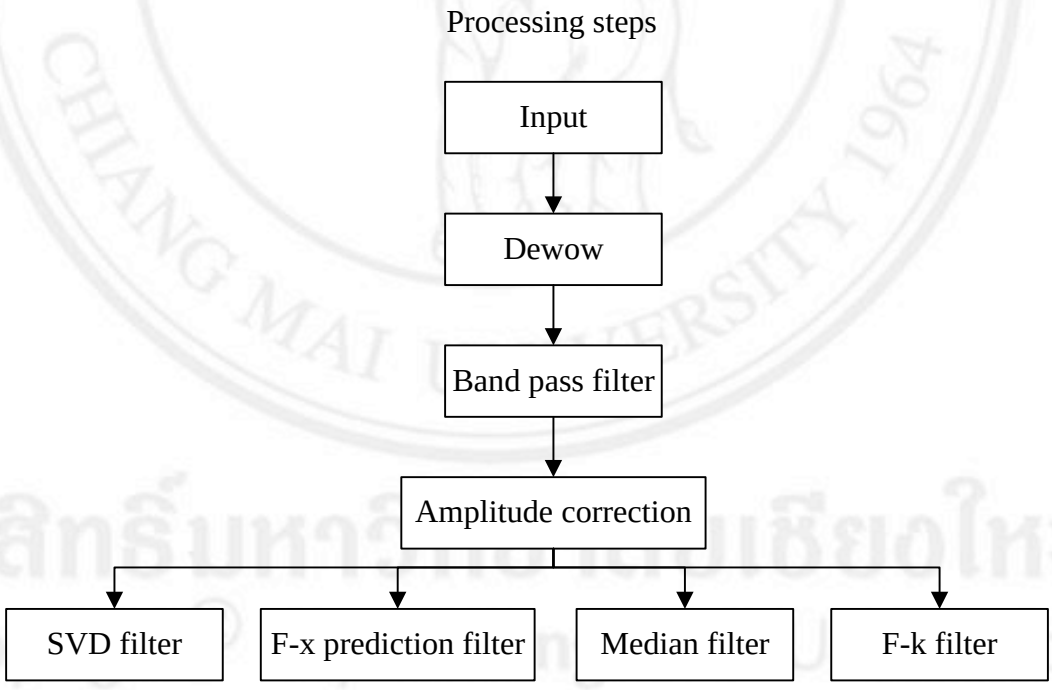

Figure 3-16. The GPR data processing steps.

Table 3-2 Processing steps and parameters of GPR data.

Processing	Parameters/remark
1. Geometry setting and trace edit	Creating header
2. Dewow	Removing DC component
3. Band pass filter	70-120-350-400 MHz
4. Amplitude correction	Automatic gain control
5. Filter testing	SVD, f-x prediction, 2-D median and f-k filters

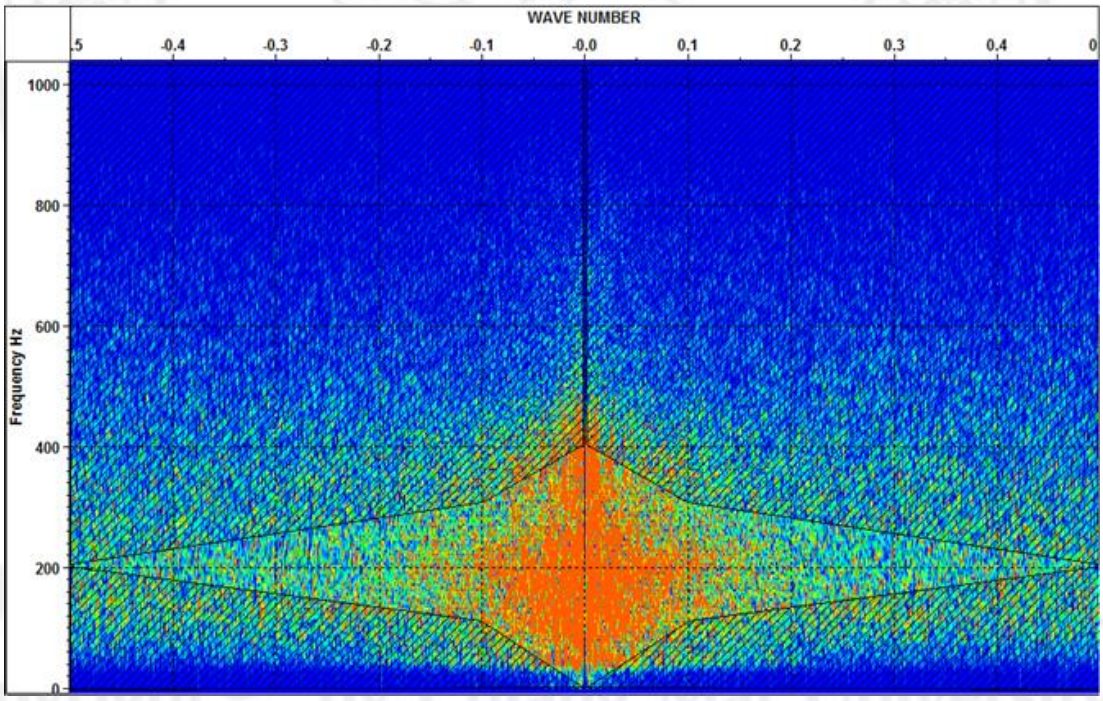

Figure 3-17. The f-k filter zone selection of GPR data.

3.2.1 Tested data set 5: GPR common offset gather

The singular value spectrum of GPR common offset gather in Figure 3-18 was divided into 3 part; p=1 to q=10 and p=10 to q=80. The test used the parameters at the range of p=1 to q=10, p=1 to q=18 and p=1 to q=44. The approximated relative magnitude at q=44 is about 0.75. The q value is not require to use q=80, because the relative magnitude less than 0.1±0.25 is not effect with filtering. The SVD filter reduced the hyperbolic events (blue arrow) and reflectors at 20 ns (red arrow). Figure 3-19c suppressed the random noise while hyperbolic events were weakly removal. Figure 3-19d was poor performance in the random noise suppression but hyperbolic events were preserved.

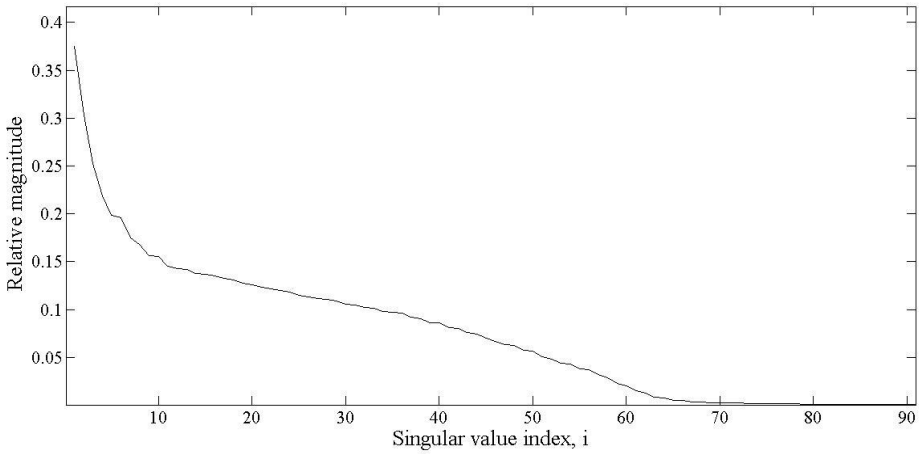

Figure 3-18. Singular value spectrum of GPR common offset gather.

The comparison results of signal enhancement using of SVD, f-x prediction, 2-D median and f-k filters were displayed in Figures 3-20a to 3-20d, respectively. Figure 3-20a shown the partially removal of hyperbolic events and the random noise at the bottom of section was remained. Figure 3-20b illustrated the clearly GRP

section and the hyperbolic events were still appeared. Figure 3-20c and Figure 3-20d were fairly performed and most of the random noises were remained but most of the signal in section was distorted.

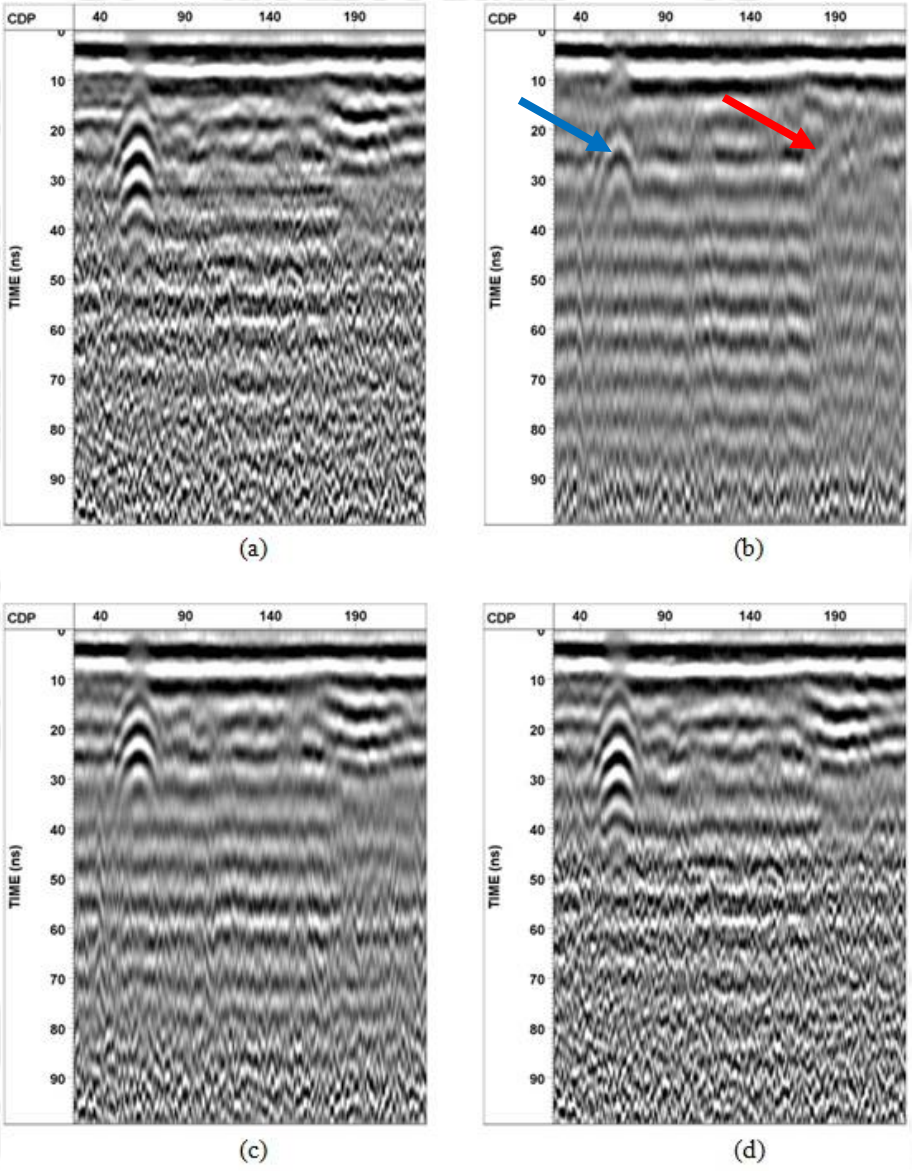

Figure 3-19. (a) Amplitude correction GPR common offset gather. (b) Amplitude correction GPR common offset gather with SVD filter using p=1 to q=10. (c) Amplitude correction GPR common offset gather with SVD filter using p=1 to q=18. (d) Amplitude correction GPR common offset gather with SVD filter using p=1 to q=44.

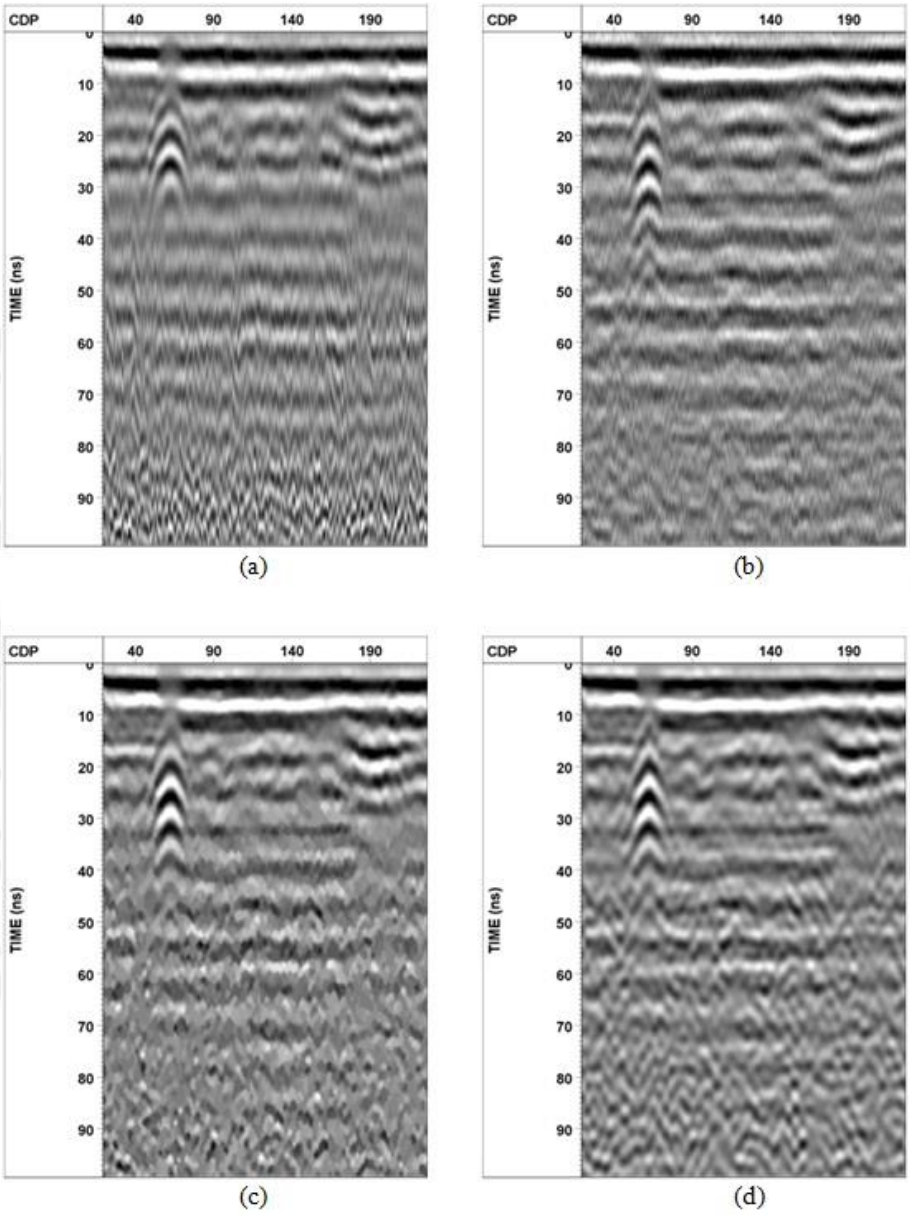

Figure 3-20. The comparison result of (a) SVD filter with p=1 to q=18, (b) f-x prediction filter with filter length of 4 traces and design windows of 48 traces, (c) 2-D median filter with window length of 3 traces and 5 samples and (d) f-k filter shape presented in Figure 3-17.

3.3 Seismic data improvement using SVD filter

The comparisons of noise suppression efficiency for each filter indicated that the SVD filter works well on CDP gather and NMO corrected CDP supergather. The seismic processing flowchart was improved and shown in Figure 3-21. Each processing steps and its parameters was presented in Table 3-3.

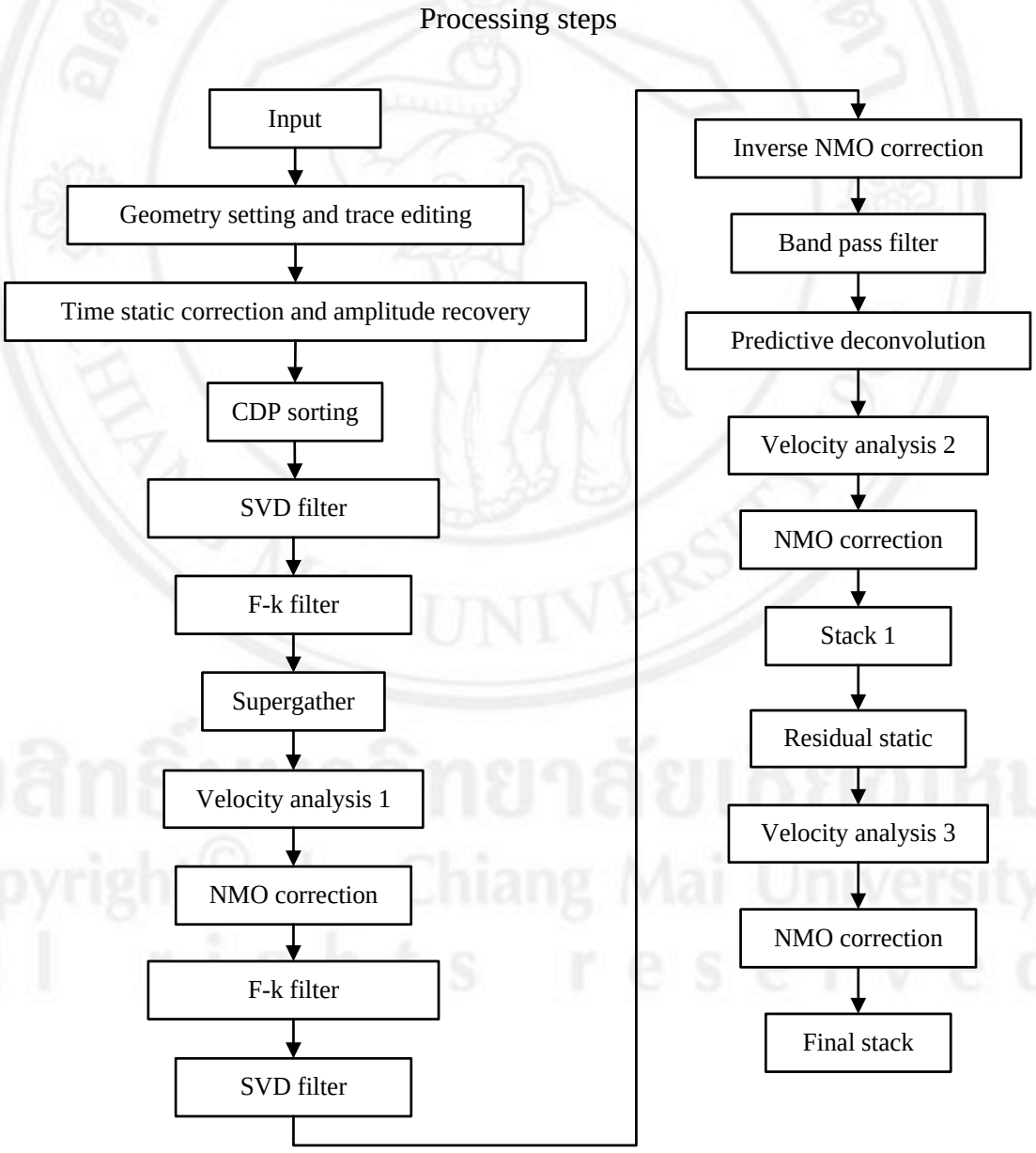

Figure 3-21. The improved seismic data processing flowchart.

Table 3-3 Processing steps (B) and parameters of seismic data.

Processing	Parameters/remark
1. Geometry setting and trace edit	
2. Time static and amplitude correction	mean scale
3. CDP sorting	
4. SVD filter	p = 3, q = 20
5. F-k filter	0-500 m/s fan shape
6. Supergather	3 CDP to 1 supergather
7. Velocity analysis 1	
8. NMO correction	
9. F-k filter	0-2500 m/s fan shape
10. SVD filter	p = 7, q = 30
11. Inverse NMO correction	
12. Band pass filter	15-25-80-90 Hz
13. Predictive deconvolution	2^{nd} crossing, n = 30 ms, ε = 0.1%
14. Velocity analysis 2	
15. NMO correction	
16. Stack 1	brute stack section
17. Residual static correction	
18. Velocity analysis 3	
19. NMO correction	
20. Final stack	final stack section

The detailed of each step was explained as follows;

Step 1: Seismic header was setup the configuration survey. The refraction wave was muted and irregular traces were killed.

Step 2: Raw data were corrected static level of source and receiver to a datum and mean scale was applied.

Step 3: Common shot gather were rearranged data for the CDP gather (Figure 3-22a).

Step 4: The ground roll was suppression by SVD filter with parameters p = 3, q = 20 (Figure 3-22b).

Step 5: The f-k filter was applied to attenuate extant ground roll and air wave (Figure 3-22c).

Step 6: The quality of seismic data were improved by the number of seismic traces in CDP gather and were increased from 24 traces to 96 traces.

Step 7: Semblance analysis, common offset stack and common velocity stack were composed velocity analysis and to obtain the velocity function.

Step 8: Velocity function in step 7 was applied for NMO correction (Figure 3-23a).

Step 9: The f-k filter was applied to random noise suppression (Figure 3-23b).

Step 10: The random noise was attenuated by the SVD filter with parameters p = 7, q = 30 (Figure 3-23c).

Step 11: Inverse NMO correction was applied using the same velocity function in step 7.

Step 12: The reflection waves were improved the quality by band pass filter.

Step 13: Predictive deconvolution was designed to eliminate multiples. All parameters were designed from autocorrelation.

Step 14: Semblance analysis, common offset stack and common velocity stack were composed velocity analysis and to obtain the velocity function (Figure 3-24).

Step 15: Velocity function in step 14 was applied for NMO correction.

Step 16: Each CDP gather was stacked and to obtain the stack section.

Step 17: When topographic correction was applied, most of small time shifts between traces remained and to correct for these small shifts the residual static correction was applied.

Step 18: Semblance analysis, common offset stack and common velocity stack were composed velocity analysis and to obtain the velocity function

Step 19: Velocity function in step 18 was applied for NMO correction.

Step 20: Each CDP gather was stacked to obtain the final stack section (Figure 3-25b).

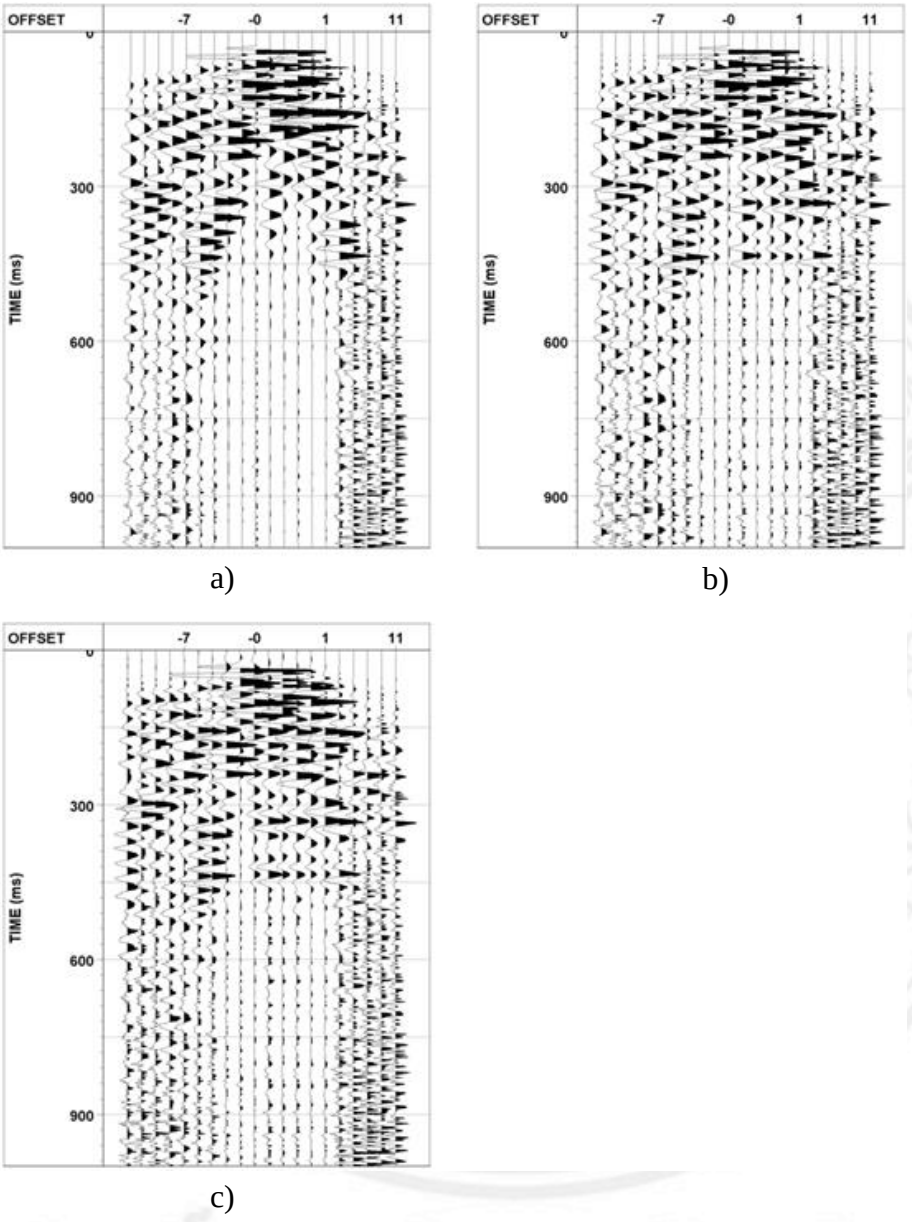

Figure 3-22. (a) CDP gather before applying SVD filter, (b) CDP gather after applied with parameters of SVD filter used p=3 to q=20. (c) CDP gather after applied f-k filter of 0-500 m/s fan shape.

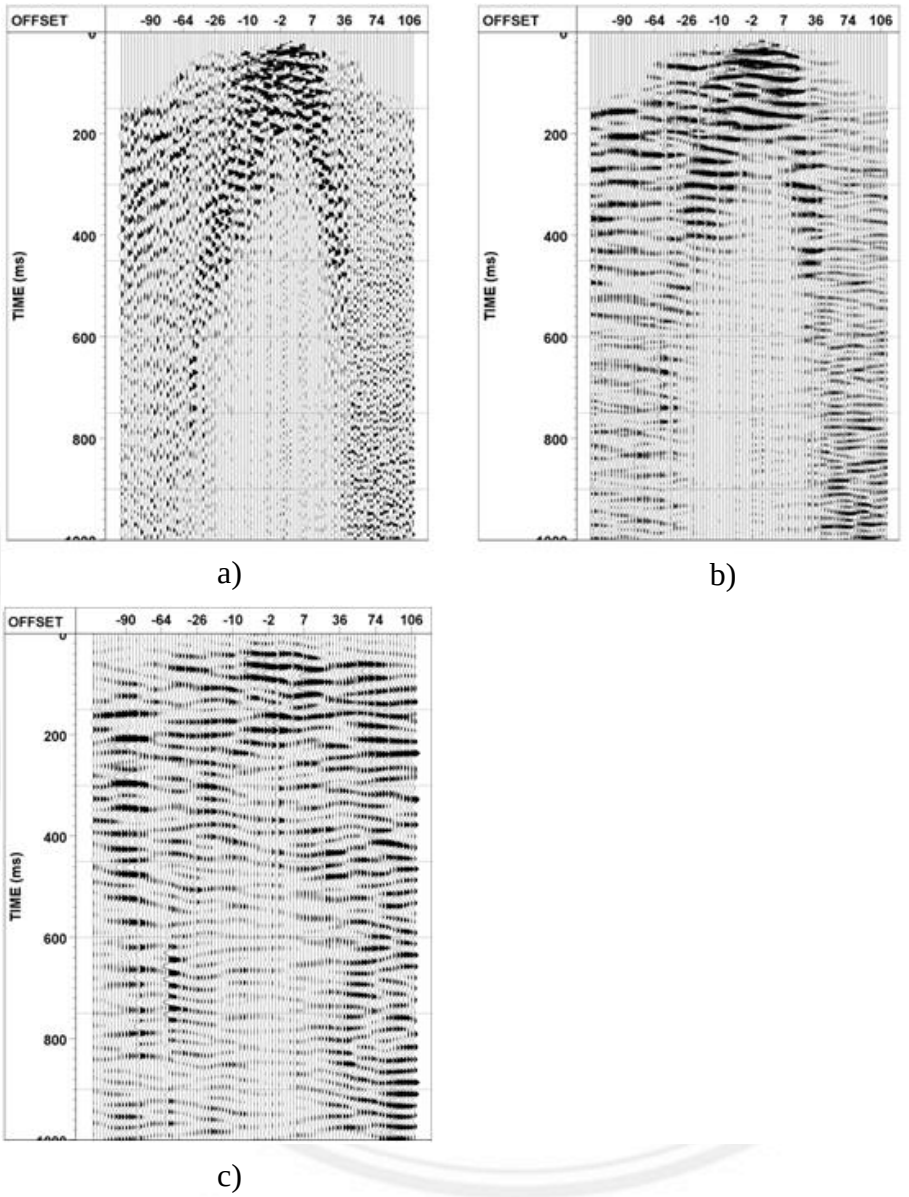

Figure 3-23. (a) NMO correction CDP supergather before applying f-k filter. (b) NMO correction CDP supergather after applied f-k filter of 0-2500 m/s fan shape. (c) NMO correction CDP supergather after applied SVD filter with parameters of SVD filter used p=7 to q=30.

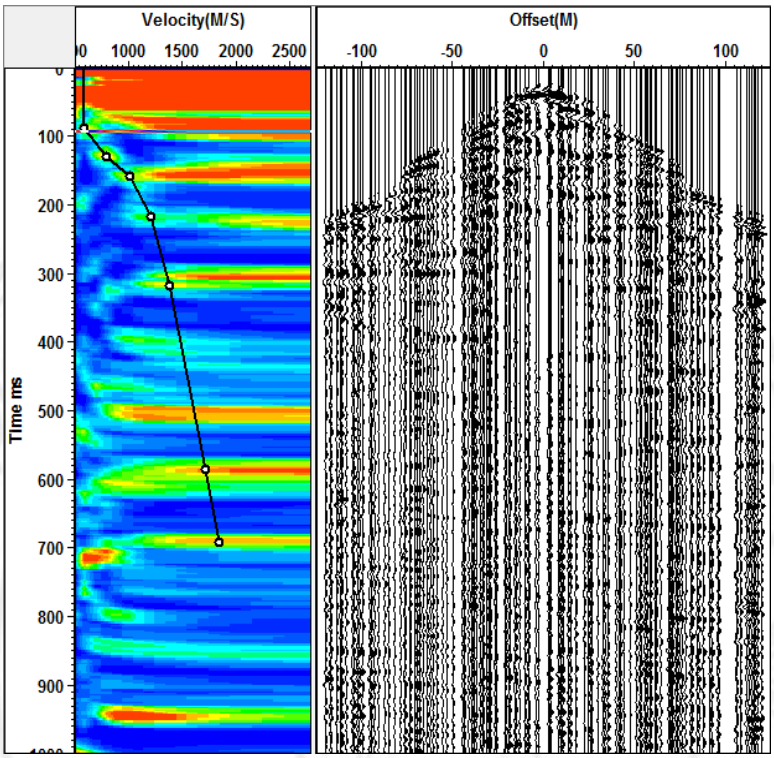

Figure 3-24. Velocity analysis, (left) the semblance analysis with the black line was velocity picking and (right) the common offset stacking.

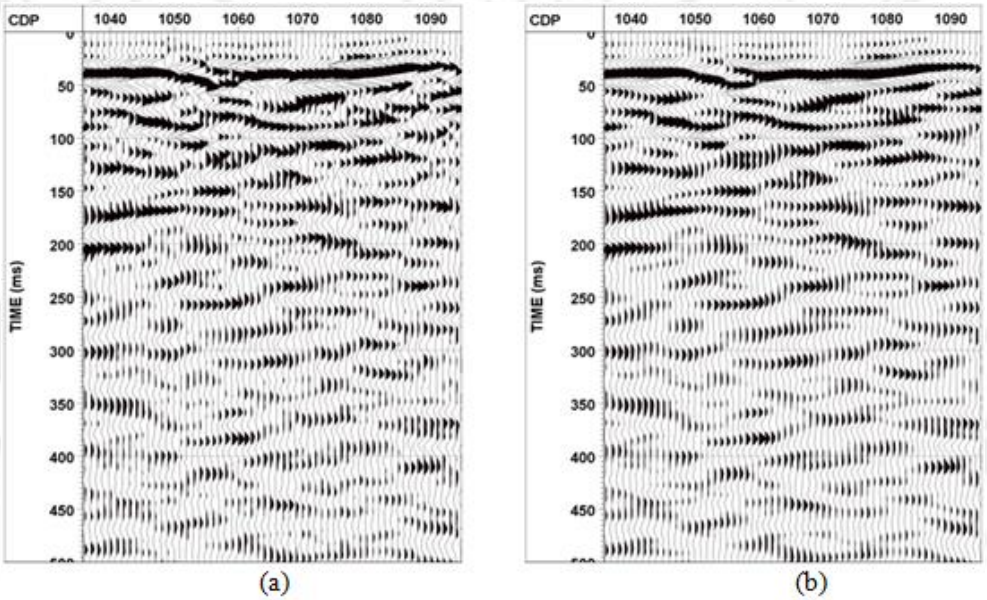

Figure 3-25. The final stack section with residual static correction, (a) from basic processing steps and (b) from improved processing steps.